2084 *Inorg. Chem.* **1995**, *34*, 2084−2088

Stoichiometry of Potassium- and Carbonate-Containing Apatites Synthesized by Solid State Reactions

Ronald M. H. Verbeeck,[*,†] **Erna A. P. De Maeyer,**[†] **and Ferdinand C. M. Driessens**[‡]

Laboratory for Analytical Chemistry, University of Ghent, Krijgslaan 281-S12, B-9000 Ghent, Belgium, and Departament de Ciència dels Materials i Enginyeria Metal-lúrgica, Universitat Politècnica de Catalunya, Barcelona, Spain

Received November 2, 1994[®]

In this study, a series of potassium- and carbonate-containing apatites is prepared by solid state reactions at high temperature in a nearly dry CO_2 atmosphere. Chemical and physical analyses showed that the samples are single-phase and contain 4−12 wt % carbonate. Their stoichiometry conforms to $Ca_{10-x}K_x[(PO_4)_{6-x}(CO_3)_x][(OH)_{2-2y}(CO_3)_y]$ with $0 < x < 1$ and $0.7 < y < 0.9$ as the result of the substitution of PO_4^{3-} as well as of OH^- by CO_3^{2-} in the apatite lattice according to the mechanisms $[Ca^{2+} + PO_4^{3-} \leftrightarrow K^+ + CO_3^{2-}]$ and $[2OH^- \leftrightarrow CO_3^{2-} + V^{OH}]$, where V^{OH} stands for a vacancy in the OH^- sublattice. Although these mechanisms appear to occur independently of each other, they have a marked effect on the IR characteristics of the solid.

Introduction

It is well-known that calcium hydroxyapatite, $Ca_{10}(PO_4)_6(OH)_2$ (HAp), can accommodate a large number of different ions in its lattice. Of these, CO_3^{2-} is generally considered the most important as it is the most abundant minor component found in apatite minerals such as francolite and dahllite as well as in the calcified tissues of higher vertebrates. The incorporation of CO_3^{2-} has considerable influence on the physical and chemical as well as physicochemical properties of the solid and hence on the mineralization, demineralization, and remineralization processes of these minerals.[1,2] The importance of such an effect becomes clear when one considers the fact that the inorganic part of calcified tissues such as bone and teeth is presumed to be entirely composed of an apatite mineral.[2] Despite numerous investigations, however, the mechanism(s) by which carbonate is incorporated in the apatite lattice is (are) not yet known or resolved in detail.[2]

It is generally accepted that CO_3^{2-} can replace OH^- as well as PO_4^{3-} ions in the apatite lattice resulting respectively in so-called A-type and B-type carbonated apatites.[2] The hexagonal crystal structure of HAp is described in detail by several authors (see ref 1 and references cited therein). Whereas the mechanism of the A-type carbonate incorporation has been well established,[3,4] the B-type incorporation apparently can involve different mechanisms.[2,5,6] In the presence of sodium ions, the carbonate incorporation in precipitated apatites on B-type sites is considerably enhanced.[7,8] This could be related to the results of recent studies[6,9] where it was found that the incorporation of B-type CO_3^{2-} in precipitated Na^+- and CO_3^{2-}- containing apatite (NCAp) is the result of two simultaneously but presumably independently occurring mechanisms represented by

$$Ca^{2+} + PO_3^{3-} + OH^- \leftrightarrow V^{Ca} + CO_3^{2-} + V^{OH} \qquad (I)$$

$$Ca^{2+} + PO_4^{3-} \leftrightarrow M^+ + CO_3^{2-} \qquad (III)$$

where $M^+ = Na^+$ and V^X stands for a vacancy on a regular apatite lattice site occupied by X. In accordance with our previous studies, these mechanisms are respectively referred to as mechanisms I and III.[5,6,9]

In the presence of K^+ instead of Na^+, K^+- and CO_3^{2-}-containing apatites (KCAp's) are precipitated which contain less carbonate and considerably less alkali metal in comparison with NCAp.[2,10,11] It is not known, however, whether the carbonate incorporation also occurs through mechanisms I and III (with $M^+ = K^+$) especially as the coupled K^+ and CO_3^{2-} incorporation according to mechanism III has not been ascertained. For this reason, the stability and stoichiometry of KCAp were investigated for those compositions favoring the occurrence of mechanism III. In order to obtain homogeneous carbonated apatites, the samples were prepared by solid state reactions at high temperatures in a nearly dry carbon dioxide atmosphere.

Experimental Section

Preparation of KCAp. For the synthesis of KCAp mixtures of reagent grade $CaHPO_4$, $CaCO_3$ and $KHCO_3$ were made so that the molar ratios of Ca, P, and K conform to $Ca/P = (10 - \alpha)/(6 - \alpha)$ and $K/Ca = \alpha/(10 - \alpha)$ with $0 \leq \alpha \leq 1$. Each mixture was homogenized by ball milling in an agate mortar for 30 min, pressed into tablets, and heated a first time at 650 °C on platinum foil in an electric tube furnace. During heating, a continuous stream of CO_2 washed over 96% sulfuric acid at room temperature was passed through the furnace tube. After 60 h of sintering at 650 °C, the products were quenched in air, powdered, and analyzed by X-ray diffraction for their phase composition. Subsequently, the samples were homogenized, pressed into

---

[†] University of Ghent.

[‡] Universitat Politècnia de Catalunya.

[®] Abstract published in *Advance ACS Abstracts,* March 15, 1995.

(1) McConnell, D. *Apatite*; Springer Verlag: Vienna, 1973.

(2) Driessens, F. C. M.; Verbeeck, R. M. H. *Biominerals*; CRC Press: Boca Raton, FL, 1990.

(3) Elliott, J. C. *Calcif. Tissue Res.* 1969, *3*, 293.

(4) Young, R. A.; Bartlett, M. L.; Spooner, S.; Mackie, P. E.; Bonel, G. *J. Biol. Phys.* 1981, *9*, 1.

(5) De Maeyer, E. A. P.; Verbeeck, R. M. H. *Bull. Soc. Chim. Belg.* 1993, *102* (9), 601.

(6) De Maeyer, E. A. P.; Verbeeck, R. M. H.; Naessens, D. E. *Inorg. Chem.* 1993, *32*, 5709.

(7) Bonel, G. *Ann. Chim.* 1972, *7*, 127.

(8) Vignoles, C.; Bonel, G.; Montel, G. *C. R. Hebd. Seances Acad. Sci., Ser. C* **1975**, *280*(6), 361.

(9) De Maeyer, E. A. P.; Verbeeck, R. M. H.; Naessens, D. E. *Inorg. Chem.* **1994**, *33*, 5999.

(10) Bonel, G.; Labarthe, J. C.; Vignoles, C. *Coll. Int. CNRS* **1975**, *230*, 117.

(11) Tomazic, B. B.; Mayer, I.; Brown, W. E. *J. Cryst. Growth* **1991**, *108*, 670.

0020-1669/95/1334-2084$09.00/0

Table 1. Chemical Composition (wt %), Density *d* (g cm^{-3}), and Lattice Parameters *a* and *c* (nm) of KCAp

sample	Ca	K	Na	P	CO_3	*d*	*a*	*c*
7	39.12	0.020	0.025	18.11	4.46	3.136	0.9508	0.6877
8	38.46	0.655	0.074	17.60	6.58	3.106	0.9509	0.6889
9	38.00	1.75	0.080	17.08	7.80	3.062	0.9477	0.6917
4	37.55	2.20	0.076	16.65	8.45	3.088	0.9452	0.6943
5	36.76	2.86	0.073	16.10	10.3	3.073	0.9445	0.6965
6	36.25	3.79	0.079	15.58	11.7	3.051	0.9441	0.6973

tablets, and heated at 750 °C for a period of 60 h. This second homogenization and sintering procedure was repeated until a constant phase composition was obtained which reflected thermodynamic equilibrium between the solid phase(s) and the gas phase at high temperature. No indications for a possible contamination from the ball milling process were found in the chemical and physical analysis results of the samples.

Chemical Analysis. The calcium content of the samples was determined by a complexometric titration with ethylenediaminetetraacetic acid[12] and the phosphorus content spectrophotometrically as the orthophosphate by using a slight modification of the method of Brabson *et al.*[13] The potassium and sodium content of the samples was determined by atomic absorption spectrophotometry. The method of Godinot *et al.*[14] was adapted for the determination of the carbonate content. The method consists of a gas chromatographic determination of the carbon dioxide evolved from an acidified aqueous solution of the apatite. The relative uncertainties in the amounts of Ca, P, CO_3, K, and Na analyzed were determined as 0.2, 0.2, 2, 2, and 4%, respectively.

Physical Analysis. X-ray powder diffraction patterns of the samples were recorded by step-scanning using a microprocessor-controlled diffractometer system (Philips PW 1830). Ni-filtered copper Kα radiation was used with an automatic divergence slit PW1836 and a graphite monochromator. The dimensions *a* and *c* of the hexagonal unit cell of the apatites were calculated from the positions of the most intense and sharp reflections (usually $n > 19$) using a least-squares refinement program. The experimental errors of *a* and *c* were estimated as 0.0006 and 0.0002 nm, respectively. IR spectra of the samples dispersed in CsBr tablets were recorded using a Mattson Galaxy 6030 Fourier transform infrared spectrophotometer. The density of the samples was measured with a helium micropycnometer of Quantachrome Corp. with an accuracy of 0.2%.

Results

Chemical Composition. Table 1 summarizes the chemical compositions of the KCAp's. The table shows that the sodium content of samples 7–9 is relatively high when compared to the potassium content and hence cannot be neglected. According to Table 1, the carbonate content of the samples increases with decreasing Ca and P content. A chemical analysis according to the method of Gee and Deitz[15] further revealed that the samples do not contain condensed phosphates within experimental error, indicating that the phosphorus is present as PO_4^{3-}.

Physical Analysis. The peaks in the X-ray diffraction patterns of the samples are sharp and well resolved and can all be attributed to the hexagonal crystal form of hydroxyapatite.[16] However, in the patterns of samples 7 and 8 some barely detectable extraneous peaks indicate the presence of β-$Ca_3(PO_4)_2$. An estimate of the amount of β-$Ca_3(PO_4)_2$ was carried out by recording the X-ray diffraction pattern of the respective KCAp sample mixed with accurately known amounts of β-$Ca_3(PO_4)_2$. On the basis of a comparison of the relative intensity of the [220] reflection of β-$Ca_3(PO_4)_2$ and the [202] reflection of the apatite, the β-$Ca_3(PO_4)_2$ contamination was estimated as 1.6 ± 0.3 wt % at the most. The effect of such an amount of second phase on the chemical composition and the density of the KCAp's can be neglected. Moreover, as this contamination has no effect on the lattice parameters of the KCAp phase, the samples can be considered as single phase.

The lattice parameters based on a hexagonal unit cell of the KCAp's are given in Table 1. It is seen that with increasing carbonate content the *a* lattice dimension decreases whereas the *c* lattice dimension increases. A weighted regression analysis indicates that this change of the lattice dimensions with the carbonate content is described at the 95% confidence level by the equations

$$a = (0.9562 \pm 0.0057) - (1.10 \pm 0.66) \times 10^{-3}[\%\ CO_3] \tag{1}$$

$$c = (0.6805 \pm 0.0045) + (1.48 \pm 0.52) \times 10^{-3}[\%\ CO_3] \tag{2}$$

Although the present samples contain some CO_3^{2-} substituting for OH^- ions (i.e. so-called A-type CO_3^{2-} as will be discussed further), the variation of the lattice dimensions according to eqs 1 and 2 is typical for a substitution of PO_4^{3-} ions by CO_3^{2-} (i.e. so-called B-type CO_3^{2-}).[2] Although the dimensions of the apatite lattice are drastically affected by the incorporation of K^+ and CO_3^{2-}, one can derive on the basis of eqs 1 and 2 that the volume of the unit cell of the KCAp's hardly changes with increasing carbonate content. Consequently, the decrease of the density with increasing carbonate and potassium content as shown in Table 1 can be ascribed merely to the exchange of Ca^{2+} and PO_4^{3-} ions by K^+ and CO_3^{2-}, respectively.

The IR spectra of the samples are typical for CO_3^{2-}-containing apatite with typical absorptions in the ranges 960–1100 and 570–610 cm^{-1} arising from PO_4^{3-} and around 875 and 1542 as well as between 1400 and 1500 cm^{-1} caused by the vibrations of CO_3^{2-} on PO_4^{3-} and OH^- lattice sites.[2] Absorptions around 3572 and 633 cm^{-1} which reflect vibrations of OH^- ions[2] are not observed. Only in the spectra of samples 4, 7, and 9 could a very weak absorption around 3572 cm^{-1} due to the stretching vibration of OH^- be detected. With increasing carbonate content, there is a drastic change of the absorption bands of CO_3^{2-}, quantitatively as well as qualitatively. This can be illustrated with Figures 1 and 2, which give respectively the 825–900 and 1300–1900 cm^{-1} regions of the IR spectra of the KCAp's.

It is seen from Figure 1 that all samples display an absorption at about 879 cm^{-1} whose intensity is nearly independent of the carbonate content. This absorption is typical for CO_3^{2-} substituting for OH^- ions in the apatite lattice (so-called A-type CO_3^{2-}).[2,20] With increasing carbonate content, an absorption at 872 cm^{-1} is observed which is due to the vibration of B-type CO_3^{2-}.[2] At a low carbonate content (sample 7), this absorption is only visible as an asymmetry of the 879 cm^{-1} band, but with increasing carbonate content, its intensity increases so that it becomes a distinct band at higher carbonate contents (see Figure 1). Figure 2 clearly shows that the absorptions in the 1300–1900 cm^{-1} region display a more complex pattern as a function

---

(12) Flaschka, H. A.; Barnard, A. J. Titrations with EDTA and related compounds. In *Comprehensive analytical chemistry*;Wilson, C. L., Wilson, D. W., Eds.; Elsevier: Amsterdam, 1960; Vol. IB.

(13) Brabson, J. A.; Dunn, R. L.; Epps, E. A.; Hoffman, W. M.; Jacobs, K. D. *J. Assoc. Off. Agric. Chem.* **1958**, *41*, 517.

(14) Godinot, C.; Bonel, G.; Torres, L.; Mathieu, J. *Microchem. J.* **1984**, *29*, 92.

(15) Gee, A.; Deitz, V. R. *J. Am. Chem. Soc.* **1955**, *77*, 2961.

(16) ASTM Powder Diffraction File No. 9–432.

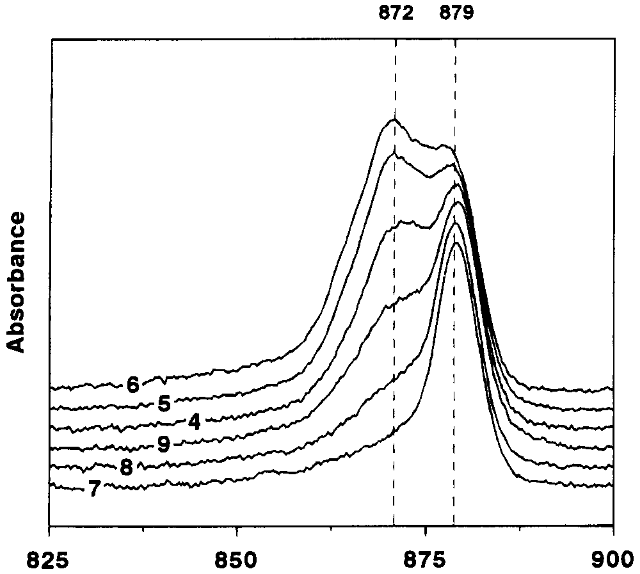

Figure 1. IR spectra of KCAp samples between 825 and 900 cm^{-1} (absorbance A versus wavenumber $\bar{\nu}$ (cm^{-1})).

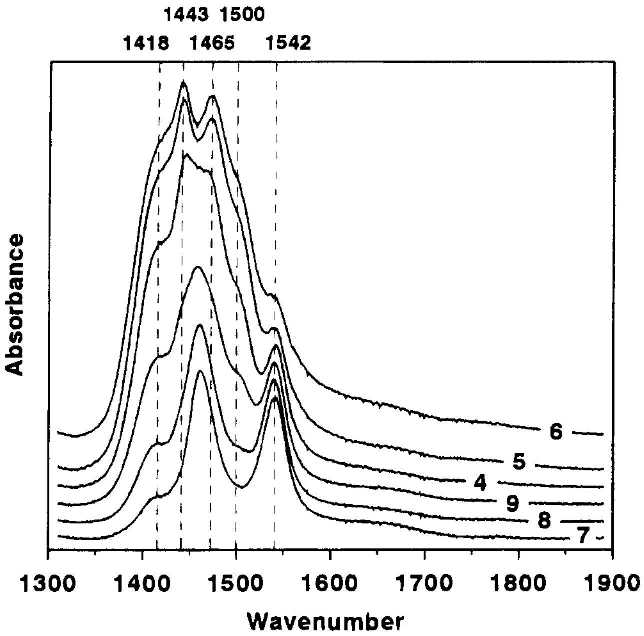

Figure 2. IR spectra of KCAp samples between 1300 and 1900 cm^{-1} (absorbance A versus wavenumber $\bar{\nu}$ (cm^{-1})).

of the carbonate content. Apart from the absorption at about 1542 cm^{-1} which is due to the vibrations of A-type carbonate,[17,18] absorptions around 1418 and 1500 cm^{-1} are seen in all spectra which can be ascribed to vibrations of B-type CO_3^{2-}.[18,19] The absorption at 1460 cm^{-1} of A-type carbonate[18] in KCAp's with a low carbonate content (samples 7–9) apparently splits into two absorptions centered around 1443 and 1465 cm^{-1} at a high carbonate content. For sample 9 (and possibly for sample 4) three absorptions can be observed; however, it is not clear whether this splitting arises from an A–B type CO_3^{2-} interaction and/or from an elongation of the unit cell (see eqs 1 and 2) or that the splitting is an artifact due to a change in the relative intensity of these absorptions with increasing carbonate content.

Discussion

As the KCAp samples are single phase, the content of the unit cell can be calculated for each sample from the data in Table 1. The results are summarized in Table 2. The errors in the number of each ion X per unit cell, n_X, were estimated by means of error propagation theory and are given in parentheses. As phosphorus is only present as PO_4^{3-}, the number of OH^- groups n_{OH} was calculated on the basis of the electroneutrality condition using the data in Table 2. According to Table 2 n_{OH} equals zero within experimental error only for samples 5 and 6, corroborating the results of the IR analysis. This indicates that some of the samples, in addition to CO_2, acquired some water during the sintering process.

n_{Ca}, n_P and the total number of alkali metal ions n_M ($=n_K + n_{Na}$) in the unit cell change linearly with each other as is illustrated with the plot of n_M versus n_P in Figure 3. This is corroborated by a weighted regression analysis which shows that at the 95% confidence level the following relationships hold

$$n_{Ca} = (3.96 \pm 0.41) + (1.000 \pm 0.074)n_P \qquad (3)$$

$$n_M = (10.0 \pm 1.2) - (1.00 \pm 0.12)n_{Ca} \qquad (4)$$

$$n_M = (6.00 \pm 0.32) - (1.008 \pm 0.058)n_P \qquad (5)$$

Moreover, the number of carbonate ions in the unit cell varies linearly with n_M, n_{Ca}, and n_P as can be illustrated with the plot of n_{CO_3} versus n_P in Figure 3. A weighted regression analysis indicates that at the 95% confidence level these relationships are given by eqs 6–8. The relationships given by eqs 3–8

$$n_{CO_3} = (0.78 \pm 0.14) + (1.16 \pm 0.24)n_M \qquad (6)$$

$$n_{CO_3} = (12.4 \pm 1.7) - (1.17 \pm 0.18)n_{Ca} \qquad (7)$$

$$n_{CO_3} = (7.8 \pm 1.0) - (1.17 \pm 0.19)n_P \qquad (8)$$

then indicate that CO_3^{2-} and the alkali metal ions are mainly incorporated in the apatite lattice on the basis of the substitution mechanism

$$Ca^{2+} + PO_4^{3-} \leftrightarrow M^+ + CO_3^{2-} \qquad (9)$$

with M = K and/or Na. The mechanism given by eq 9 is in line with observations[2,6,9,20,21] that CO_3^{2-} substitutes for PO_4^{3-} on a 1:1 mole basis so that the phosphate lattice sites in apatite remain fully occupied, i.e.

$$n_P + n_{B\text{-}CO_3} = 6 \qquad (10)$$

where $n_{B\text{-}CO_3}$ then represents the number of B-type CO_3^{2-} in the unit cell.

The facts that according to eq 8 and Table 2 n_{CO_3} is substantially greater than n_M and that the sum of n_P and n_{CO_3} is always greater than 6 indicate that some carbonate must be incorporated by a mechanism differing from that given by eq 9. This is corroborated by the IR analysis which shows that part of the carbonate is present as A-type carbonate, i.e

---

(17) Elliott, J. C.; Holcomb, D. W.; Young, R. A. *Calcif. Tissue Int.* **1985**, *37*, 372.

(18) Rey, C.; Collins, B.; Goehl, T.; Dickson, I. R.; Glimcher, M. J. *Calcif. Tissue Int.* **1989**, *45*, 157.

(19) Shimoda, S.; Aoba, T.; Moreno, E. C.; Miake, Y. *J. Dent. Res.* **1990**, *69*, 1731.

(20) Driessens, F. C. M.; Verbeeck, R. M. H.; Heijligers, H. J. M. *Inorg. Chim. Acta* **1983**, *80*, 19.

(21) Driessens, F. C. M.; Verbeeck, R. M. H.; Kiekens, P. *Z. Anorg. Allg. Chem.* **1983**, *504*, 195.

Table 2. Content of the Unit Cell of KCAp Calculated on the Basis of the Data in Table 1 (Calculated Uncertainties Given in Parentheses)

sample	n_{Ca}	n_P	n_{CO_3}	n_K	n_{Na}	n_{OH}	$n_{B\text{-}CO_3}$	$n_{A\text{-}CO_3}$	$n_V{}^{Ca}$	$n_V{}^{OH}$
7	9.923 (0.028)	5.944 (0.017)	0.756 (0.015)	0.0052 (0.0001)	0.0111 (0.0004)	0.518 (0.081)	0.056 (0.017)	0.700 (0.023)	0.061 (0.028)	0.080 (0.076)
8	9.682 (0.028)	5.733 (0.017)	1.106 (0.022)	0.1690 (0.0034)	0.0325 (0.0013)	0.155 (0.088)	0.267 (0.017)	0.839 (0.028)	0.117 (0.028)	0.168 (0.090)
9	9.407 (0.029)	5.471 (0.017)	1.290 (0.026)	0.4432 (0.0090)	0.0345 (0.0014)	0.299 (0.094)	0.529 (0.017)	0.761 (0.031)	0.115 (0.030)	0.179 (0.094)
4	9.359 (0.027)	5.373 (0.016)	1.407 (0.028)	0.562 (0.011)	0.0330 (0.0013)	0.380 (0.092)	0.627 (0.016)	0.780 (0.032)	0.046 (0.029)	0.058 (0.099)
5	9.132 (0.026)	5.176 (0.015)	1.709 (0.034)	0.728 (0.015)	0.0316 (0.0013)	0.078 (0.098)	0.824 (0.015)	0.885 (0.037)	0.108 (0.030)	0.15 (0.12)
6	8.945 (0.027)	4.975 (0.015)	1.928 (0.039)	0.959 (0.019)	0.0340 (0.0014)	0.10 (0.11)	1.025 (0.015)	0.903 (0.042)	0.062 (0.033)	0.09 (0.13)

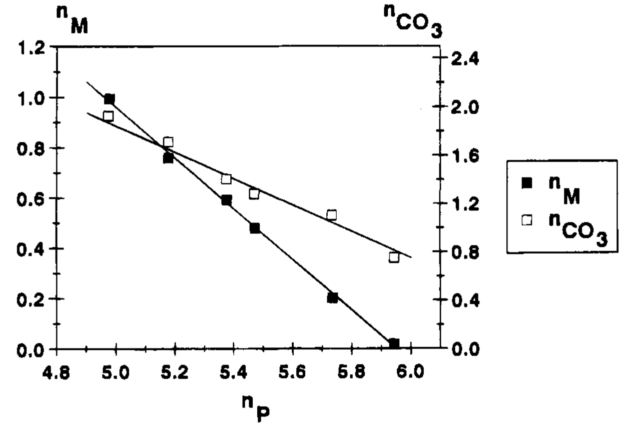

Figure 3. Number of K^+ and Na^+ ions (n_M) and number of $CO_3{}^{2-}$ ions (n_{CO_3}) versus the number of phosphate ions (n_P) in the unit cell of KCAp.

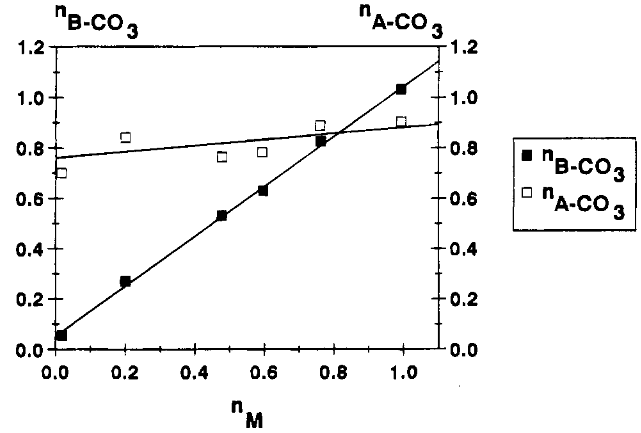

Figure 4. Number of carbonate ions on B-type sites ($n_{B\text{-}CO_3}$) and on A-type sites ($n_{A\text{-}CO_3}$) versus the number of alkali metal ions (n_M; M = K + Na) in the unit cell of KCAp.

$CO_3{}^{2-}$ ions which substitute OH^- ions according to the mechanism[2-5]

$$2OH^- \leftrightarrow CO_3{}^{2-} + V^{OH} \qquad (11)$$

In eq 11 V^{OH} represents a vacancy on a regular apatite lattice site normally occupied by OH^-. The number of A-type $CO_3{}^{2-}$ ions in the unit cell, $n_{A\text{-}CO_3}$, as well as $n_{B\text{-}CO_3}$ can be calculated easily using eqs 10 and 12 and the values for n_P and n_{CO_3} given in Table 2. The result of this calculation is summarized in

$$n_{CO_3} = n_{B-CO_3} + n_{A-CO_3} \qquad (12)$$

columns 8 and 9 of Table 2. Table 2 shows that $n_{B\text{-}CO_3}$ increases with increasing n_{CO_3} and n_M, whereas $n_{A\text{-}CO_3}$ hardly changes with the composition of KCAp. This can be clearly illustrated with a plot of $n_{B\text{-}CO_3}$ and $n_{A\text{-}CO_3}$ versus n_M as shown in Figure 4. A weighted regression analysis further reveals that at the 95% confidence level the following relationships hold

$$n_{B-CO_3} = (0.053 \pm 0.034) + (0.990 \pm 0.057)n_M \qquad (13)$$

$$n_{B-CO_3} = (9.93 \pm 0.70) - (0.997 \pm 0.074)n_{Ca} \qquad (14)$$

As the intercept of eq 13 differs significantly from zero for $n_M = 0$, this could be an indication that some B-type $CO_3{}^{2-}$ might be incorporated by a mechanism differing from that given by eq 9. This could be substantiated when the number of vacancies on Ca^{2+} and OH^- lattice sites, respectively given by eqs 15 and 16, are considered by taking into account the

$$n_V{}^{Ca} = 10 - n_{Ca} - n_M \qquad (15)$$

$$n_V{}^{OH} = 2 - 2n_{A-CO_3} - n_{OH} \qquad (16)$$

occurrence of A-type $CO_3{}^{2-}$ (eq 11) and B-type $CO_3{}^{2-}$ according to eq 9. The two last columns in Table 2 indicate that the values for $n_V{}^{Ca}$ and $n_V{}^{OH}$ are positive and that $n_V{}^{Ca} \approx n_V{}^{OH}$ within experimental error. This observation could be accounted for by the occurrence of the substitution mechanism

$$Ca^{2+} + PO_4{}^{3-} + OH^- \leftrightarrow V^{Ca} + CO_3{}^{2-} + V^{OH} \qquad (17)$$

according to which $CO_3{}^{2-}$ substitutes for $PO_4{}^{3-}$ on a 1:1 basis with the simultaneous creation of a vacancy on the Ca^{2+} and OH^- lattice sites of apatite.

On the other hand, the fact that $n_V{}^{Ca} \approx n_V{}^{OH} > 0$ could be an artifact due to the sintering process. During this process isolated microvoids can be created within the particles, resulting in an underestimation of the density. Consequently, n_{Ca}, n_P, n_{CO_3}, and n_M as well as n_{OH} would be underestimated, whereas $n_{B\text{-}CO_3}$ and $n_{A\text{-}CO_3}$ would be respectively too high and too low, resulting in an overestimation of $n_V{}^{Ca}$ and $n_V{}^{OH}$. For hydroxyapatite obtained by sintering at an appropiate temperature and for a sufficient time, the volume occupied by isolated micropores usually ranges from 0 to 5 vol%.[22] Assuming that a microporosity of 1 vol% occurs, one can calculate e.g. for sample 9 that $n_V{}^{Ca}$ and $n_V{}^{OH}$ would amount to respectively 0.017 and 0.042 instead of 0.115 and 0.179 (see Table 2). As the former values for $n_V{}^{Ca}$ and $n_V{}^{OH}$ equal zero within experimental error and in view of the fact that $n_V{}^{Ca}$ and $n_V{}^{OH}$ do not change systematically with the carbonate and potassium content of the KCAp's, the occurrence of such microporosities more likely explains the apparent vacancies on the Ca^{2+} and OH^- lattice sites than the occurrence of the substitution mechanism represented by eq 17. On this basis, the stoichiometry of KCAp

---

[22] de Groot, K. *Bioceramics of Calcium Phosphate*; CRC Press: Boca Raton, FL, 1983; p 99.

prepared at high temperatures as in the present study can be totally accounted for by the occurrence of the substitution mechanisms given by eqs 9 and 11 resulting in the formula

$$Ca_{10-x}K_x[(PO_4)_{6-x}(CO_3)_x][(OH)_{2-2y}(CO_3)_y] \quad (18)$$

Although the data in Table 2 suggest that $n_{A\text{-}CO_3}$ tends to increase with increasing $n_{B\text{-}CO_3}$, a correlation between these two quantities is statistically not significant ($0.10 < p < 0.25$). Consequently, an interaction between the mechanisms represented by eqs 9 and 11 resulting in a change of their relative contributions to the carbonate incorporation will be very small or nonexistent. Moreover, as $n_{A\text{-}CO_3}$ remains nearly constant over the composition range investigated in this study (see Figure 4 and Table 2) and the number of CO_3^{2-} ions substituting for PO_4^{3-} ions is restricted to 1:6 at the most (see $n_{B\text{-}CO_3}$ in Table 2), the splitting of the 1460 cm^{-1} absorption band (see Figure 2) is not likely to be caused by an interaction between A- and B-type CO_3^{2-}. Whether this is an effect of a change in lattice dimensions or is caused by a change in the relative intensity of the A-type and B-type CO_3^{2-}absorptions with increasing carbonate content should be more specifically investigated.

On the basis of (18) and the values for x and y which correspond respectively to $n_{B\text{-}CO_3}$ and $n_{A\text{-}CO_3}$ in Table 2, one can estimate the effect of the coupled (K^+, CO_3^{2-}) incorporation according to eq 9 and that of the A-type carbonate incorporation (eq 11) on the lattice parameters of HOAp. A multiple regression analysis shows that at the 95% confidence level the variation of a and c (see Table 1) as a function of x and y is given respectively by

$$a = (0.9418 \pm 0.0018) - (0.0106 \pm 0.0020)x + (0.0139 \pm 0.0026)y \quad (19)$$

and

$$c = (0.6882 \pm 0.0020) + (0.0106 \pm 0.0022)x - (0.0016 \pm 0.0028)y \quad (20)$$

The extreme compositions of (18) $\{x = 0; y = 0\}$ and $\{x = 0; y = 1\}$ corresponding respectively to hydroxyapatite and pure A-type carbonate apatite were included in this analysis. For the former $a = 0.9418$ nm and $c = 0.6884$ nm,[16] whereas for the latter $a = 0.9557$ nm and $c = 0.6872$ nm.[23] Equation 19 shows that both the coupled (K^+, CO_3^{2-}) incorporation (eq 9) and the A-type CO_3^{2-} incorporation (eq 11) have drastic but opposite effects on the a lattice dimension. The variation of a with y compares with that calculated from the literature, i.e. $da/dy = +0.015$ nm.[24] According to eq 20, the effect of the coupled (K^+, CO_3^{2-}) incorporation on the c dimension is comparable in magnitude but opposite to that on the a lattice dimension. Apparently, the A-type CO_3^{2-} incorporation does not significantly affect the c lattice dimension. This is not surprising in view of the small difference of c between HOAp and pure A-type carbonate apatite on the one hand and the experimental error in this parameter on the other hand.

When a multiple regression analysis is performed on the data for NCAp's prepared by solid state reactions at high temperatures,[20] one finds that at the 95% confidence level the lattice dimensions change as a function of x and y according to eqs 21 and 22. These equations show that the effect on the a lattice dimension of a coupled (Na^+, CO_3^{2-}) incorporation according to eq 9 is similar to that found for KCAp's. However, the c dimension is significantly less influenced by such incorporation when compared to the (K^+, CO_3^{2-}) incorporation (eq 20). Consequently, the hexagonal unit cell of the apatite lattice will become less elongated in the c axis direction when B-type CO_3^{2-} is incorporated in the presence of Na^+.

$$a = (0.9403 \pm 0.0049) - (0.0131 \pm 0.0041)x + (0.0141 \pm 0.0070)y \quad (21)$$

$$c = (0.6890 \pm 0.0020) + (0.0047 \pm 0.0017)x - (0.0016 \pm 0.0029)y \quad (22)$$

Conclusions

The stoichiometry of KCAp prepared by solid state reactions at high temperature under a CO_2 atmosphere conforms to that of HAp in which the lattice ions are substituted by K^+ and CO_3^{2-} according to the mechanisms [$Ca^{2+} + PO_4^{3-} \leftrightarrow K^+ + CO_3^{2-}$] and [$2OH^- \leftrightarrow CO_3^{2-} + V^{OH}$]. These results then confirm that a coupled incorporation of CO_3^{2-} and K^+ in a 1:1 mole ratio in HAp can occur as is the case for Na^+ and CO_3^{2-}. The difference in size between K^+ and Na^+ most probably is responsible for some small differences in the physical properties of K^+- and Na^+-containing carbonated apatites.

Acknowledgment. This work is part of a project supported by the "Executieve van de Vlaamse Gemeenschap—Departement Onderwijs", which is gratefully acknowledged.

IC9412668

---

(23) Elliott, J. C.; Bonel, G.; Trombe, J. C. *J. Appl. Cryst.* **1980**, *13*, 618.

(24) Young, R. A.; Holcomb, D. W. *Calcif. Tissue Int.* **1982**, *34*, S17.